

Electron–phonon interaction and optical spectra of metals

H. J. Kaufmann*

Interdisciplinary Research Centre in Superconductivity, University of Cambridge, Madingley Road, Cambridge CB3 0HE, UK and Department of Earth Sciences, University of Cambridge, Downing Street, Cambridge CB2 3EQ, UK.

E. G. Maksimov

P. N. Lebedev Physical Institute, 117924 Moscow, Russia.

E. K. H. Salje

Interdisciplinary Research Centre in Superconductivity, University of Cambridge, Madingley Road, Cambridge CB3 0HE, UK and Department of Earth Sciences, University of Cambridge, Downing Street, Cambridge CB2 3EQ, UK.

Abstract

Observed optical reflectivity in the infrared spectral region is compared with theoretical predictions in a strongly coupled electron–phonon system. Starting from a Fröhlich Hamiltonian, the spectral functions and their temperature dependence are derived. A full analysis including vertex corrections leads to an expression for the optical conductivity $\sigma(\omega)$ which can be formulated in terms of the well known optical conductivity for a quasi–isotropic system without vertex corrections. A numerical comparison between the full result and the so–called “extended” Drude formula, its weak coupling expansion, show little difference over a wide range of coupling constants. Normal state optical spectra for the high- T_c superconductors $\text{YBa}_2\text{Cu}_3\text{O}_7$ and $\text{La}_{2-x}\text{Sr}_x\text{CuO}_4$ at optimal doping are compared with the results of model calculations. Taking the plasma frequency and ϵ_∞ from band structure calculations, the model has only one free parameter, the electron–phonon coupling constant λ . In both materials the overall behaviour of the reflectivity can be well accounted for over a wide frequency range. Systematic differences exist only in the mid–infrared region. They become more pronounced with increasing frequency, which indicates that a detailed model for the optical response should include temperature dependent mid–infrared bands.

Keywords: optical properties, electron–phonon interaction, high- T_c superconductors

Typeset using REVTeX

*corresponding author; Tel. +44-1223-333409, Fax +44-1223-333450, e-mail hjk22@cus.cam.ac.uk

I. INTRODUCTION

The optical spectra of metals in the infrared (IR) spectral region depend sensitively on the interaction between electrons and phonons. Deviations from the theoretical spectrum without any phonon contribution stem from the so-called Holstein mechanism [1] in which the incident photon is absorbed in a second-order process involving creation of both a phonon and an electron-hole pair. The detailed description of this mechanism was given by Allen [2]. Despite the fact that the physical mechanism of electron-phonon coupling is rather well understood for almost three decades, little progress was made in the systematic experimental study of coupling effects in optical (IR) spectra [3], nor has the phenomenology been explored beyond the lowest order effects. The lack of systematic experimental investigations appears to be related to the following two reasons:

Firstly, historically measurements of optical spectra of metals were limited to photon energies $\omega \gtrsim 0.05$ eV [3]. We shall argue in this paper that the effects of the electron-phonon interaction on the optical spectra of ordinary metals are rather weak at these energies. The optical conductivity in this spectral range can usually be described in the framework of the Drude formula

$$\sigma(\omega) = \frac{\omega_{\text{pl}}^2}{4\pi} \frac{1}{-i\omega + 1/\tau} \quad (1)$$

where $1/\tau$ is the relaxation rate of electrons due to their interaction with impurities and phonons. It can be calculated using the commonly adapted Bloch-Grüneisen-type formula.

Secondly, the measurements of the optical conductivity are complicated in ordinary metals by the anomalous skin effect which is mostly present at low temperatures and in the far-infrared (FIR) spectral region. It leads to serious difficulties in the interpretation of reflectivity and absorptivity measurements. Only a few observations [4,5] are known to us where Holstein processes were identified in the normal state of ordinary metals.

The discovery of the high- T_c superconductors (HTSC) has dramatically changed the experimental situation. First of all, the experimental methods were improved radically by extending the accessible energy range down to ≈ 10 cm $^{-1}$ and by increasing the accuracy of the measurements. Secondly, it appears that HTSC systems allow the observation of the electron-phonon interaction in the optical spectra more easily and more clearly than it was possible in the ordinary metals. Thirdly, there is no anomalous skin effect in these systems for light with electric field parallel to the Cu-O planes.

It is the purpose of this paper to review the theoretical situation. We then extend the treatment of the Fröhlich Hamiltonian to include vortex corrections. Theoretical predictions are then compared with experimental observations following earlier attempts to connect the IR reflectivity and absorption spectra of HTSCs with features of strongly interacting electron-phonon systems [6-8].

We shall show that most but not all observations can be described rather well within such a scheme and identify some pertinent open questions.

II. DERIVATION OF THE OPTICAL CONDUCTIVITY IN THE FRAMEWORK OF THE FRÖHLICH HAMILTONIAN

We start from the description of metals with electron–phonon interaction by the standard Fröhlich Hamiltonian

$$H = \sum_{\mathbf{k},i} \epsilon_{\mathbf{k},i} c_{\mathbf{k},i}^\dagger c_{\mathbf{k},i} + \sum_{\mathbf{k},\mathbf{q},i,i',\lambda} g_{\mathbf{k}}(\mathbf{q}, i, i', \lambda) c_{\mathbf{k},i}^\dagger c_{\mathbf{k}+\mathbf{q},i'} \times \quad (2)$$

$$\times \left(b_{\mathbf{q}\lambda}^\dagger + b_{-\mathbf{q}\lambda} \right) + \sum_{\mathbf{q},\lambda} \omega_{\mathbf{q}\lambda} b_{\mathbf{q}\lambda}^\dagger b_{\mathbf{q}\lambda} .$$

Here the first term is the kinetic energy of an electron with given momentum \mathbf{k} and band index i , the last term is the energy of the phonon with momentum \mathbf{q} and mode λ . The second term represents the electron–phonon interaction, where $g_{\mathbf{k}}(\mathbf{q}, i, i', \lambda)$ is the matrix element of this interaction. The use of this Hamiltonian for the self-consistent calculation of the electron and phonon Green’s functions cannot be rigourously justified in the general case. It was shown [9–11] that this Hamiltonian can be used for the calculation of the influence of the electron–phonon interaction on the electronic properties for systems where no low-energy collective excitations of electrons are present. First-principle calculations [10] of the physical properties of a number of ordinary metals have shown that the Fröhlich Hamiltonian is a very good starting point for the analysis of all features related to electron–phonon interactions. In HTSC materials we can not expect this Hamiltonian to describe the optical response completely because additional low energy excitations (e.g. spin and/or charge excitations) occur. However, these excitations contribute little to the general trend of the “anomalous” optical properties of HTSC systems at high energies and are simply ignored in this study. The question we wish to answer here is the following: to what extent can observed optical spectra in the normal state be understood in terms of the most simple model of electron–phonon interaction as represented by equation (2).

The many-body electron–phonon interaction are usually calculated by Green’s function method [12]. Let us introduce the electron and phonon one-particle thermodynamic Green’s functions

$$G_i(\mathbf{k}, \tau) = -\langle T_\tau c_{\mathbf{k},i}^\dagger(\tau) c_{\mathbf{k},i}(0) \rangle \quad (3)$$

and

$$D_\lambda(\mathbf{q}, \tau) = -\langle T_\tau b_{\mathbf{q}\lambda}^\dagger(\tau) b_{\mathbf{q}\lambda}(0) \rangle . \quad (4)$$

The Wick operator T_τ reorders the operators following it in such a way that τ increases from right to left. For non-interacting particles the Fourier components of the Green’s functions, $G_i(\mathbf{k}, i\omega_n)$ and $D_\lambda(\mathbf{q}, i\omega_\nu)$, have the very simple form

$$G_i^0(\mathbf{k}, i\omega_n) = \frac{1}{i\omega_n - \epsilon_{\mathbf{k},i}} \quad (5)$$

and

$$D_\lambda^0(\mathbf{q}, i\omega_\nu) = \left(\frac{1}{i\omega_\nu - \omega_{\mathbf{q}\lambda}} - \frac{1}{i\omega_\nu + \omega_{\mathbf{q}\lambda}} \right) . \quad (6)$$

Here $i\omega_n = (2n + 1)\pi T$ and $i\omega_\nu = 2\nu\pi T$ are the Matsubara frequencies for fermions and bosons, respectively, and T is the temperature. The value $\epsilon_{\mathbf{k},i}$ is the electron band energy and, correspondingly, $\omega_{\mathbf{q}\lambda}$ is the phonon energy for the λ th mode. In the following we do not consider the renormalisation of the phonon Green's function due to the electron-phonon interaction. For convenience we present the phonon function $D_\lambda(\mathbf{q}, i\omega_\nu)$ in the spectral form

$$D_\lambda(\mathbf{q}, i\omega_\nu) = \frac{1}{\pi} \int_0^\infty d\Omega \operatorname{Im} D_\lambda(\mathbf{q}, \Omega) \left(\frac{1}{i\omega_\nu - \Omega} - \frac{1}{i\omega_\nu + \Omega} \right). \quad (7)$$

For the non-interacting case the spectral density $\operatorname{Im} D_\lambda(\mathbf{q}, \Omega)$ has the form

$$\operatorname{Im} D_\lambda^0(\mathbf{q}, \Omega) = \pi \delta(\Omega - \omega_{\mathbf{q}\lambda}). \quad (8)$$

In the following we treat the spectral function $\operatorname{Im} D_\lambda(\mathbf{q}, \Omega)$ as an experimental quantity and calculate the influence of the electron-phonon interaction on the electronic properties. These properties are reflected in the one-particle electron Green's function and the optical conductivity $\sigma_{\alpha\beta}(\omega)$. The one-particle Green's function for electrons in the presence of the electron-phonon interaction [13] can be written as

$$G^{-1}(\mathbf{k}, i\omega_n) = G_0^{-1}(\mathbf{k}, i\omega_n) - \Sigma(\mathbf{k}, i\omega_n) \quad (9)$$

where $\Sigma(\mathbf{k}, i\omega_n)$ is the electron self-energy part. One of the main results of Migdal [13] is that the electron self-energy can be calculated using the simplest first-order approximation in the electron-phonon interaction, neglecting all vertex corrections as being small of the order of ω_D/ϵ_F . Here ω_D is a characteristic phonon energy and ϵ_F is the Fermi energy of the electrons. An analytical expression of $\Sigma(\mathbf{k}, i\omega_n)$ is

$$\begin{aligned} \Sigma_i(\mathbf{k}, i\omega_n) = & -T \sum_{\omega_\nu} \sum_{\mathbf{k}', i', \lambda} |g_{\mathbf{k}}(\mathbf{k} - \mathbf{k}', i, i', \lambda)|^2 D_\lambda(\mathbf{k} - \mathbf{k}', i\omega_\nu) \times \\ & \times G(\mathbf{k}', i\omega_n - i\omega_\nu). \end{aligned} \quad (10)$$

The summation over the momentum \mathbf{k}' is represented in integral form

$$\sum_{\mathbf{k}, i} = \sum_i \int_{-\infty}^{\infty} d\epsilon \sum_{\mathbf{k}} \delta(\epsilon - \epsilon_{\mathbf{k},i}) \quad (11)$$

so that $\Sigma_i(\mathbf{k}, i\omega_n)$ becomes

$$\begin{aligned} \Sigma_i(\mathbf{k}, i\omega_n) = & -T \sum_{\omega_\nu} \int_{-\infty}^{\infty} d\epsilon \sum_{\mathbf{k}', i', \lambda} |g_{\mathbf{k}}(\mathbf{k} - \mathbf{k}', i, i', \lambda)|^2 \delta(\epsilon - \epsilon_{\mathbf{k}', i'}) \times \\ & \times \int_0^\infty d\Omega \operatorname{Im} D_\lambda(\mathbf{k} - \mathbf{k}', \Omega) G(\mathbf{k}', i\omega_n - i\omega_\nu) \times \\ & \times \left(\frac{1}{i\omega_\nu - \Omega} - \frac{1}{i\omega_\nu + \Omega} \right). \end{aligned} \quad (12)$$

The analysis of (12), as performed by Migdal, shows that the essential values of $i\omega_n$ and $i\omega_\nu$ are of order ω_D . This means that small frequencies of order ω_D are also significant for ϵ . In

this case ϵ can be neglected in $\delta(\epsilon - \epsilon_{\mathbf{k},i})$. The electron Green's function is used in the form given by Eq. (5) leading to

$$\begin{aligned} \Sigma_i(\mathbf{k}, i\omega_n) = & -T \sum_{\omega_\nu} \sum_{\mathbf{k}'} \delta(\epsilon_{\mathbf{k}'}) \int_0^\infty d\Omega \alpha_i^2(\mathbf{k}, \mathbf{k}', \Omega) F(\Omega) \left(\frac{1}{i\omega_\nu - \Omega} - \frac{1}{i\omega_\nu + \Omega} \right) \times \\ & \times \int_{-\infty}^\infty d\epsilon \frac{1}{i\omega_n - i\omega_\nu - \epsilon}, \end{aligned} \quad (13)$$

where the spectral function of the electron-phonon interaction

$$\alpha_i^2(\mathbf{k}, \mathbf{k}', \Omega) F(\Omega) = \sum_{i', \lambda} |g_{\mathbf{k}}(\mathbf{k} - \mathbf{k}', i, i', \lambda)|^2 \text{Im } D_\lambda(\mathbf{k} - \mathbf{k}', \Omega) \quad (14)$$

was introduced. The sum over the $\omega_\nu = 2\pi\nu T$ can be easily performed with the result

$$\begin{aligned} -T \sum_{\omega_\nu} \left(\frac{1}{i\omega_\nu - \Omega} - \frac{1}{i\omega_\nu + \Omega} \right) \frac{1}{i\omega_n - i\omega_\nu - \epsilon} = \\ = \frac{N(\Omega) + 1 - f(\epsilon)}{i\omega_n - \Omega - \epsilon} + \frac{N(\Omega) + f(\epsilon)}{i\omega_n + \Omega - \epsilon}, \end{aligned} \quad (15)$$

where $N(\Omega)$ and $f(\epsilon)$ are the Bose and Fermi function, respectively. To obtain the one-particle Green's function describing the electron excitation spectrum we use the analytic continuation of the self-energy on the imaginary axis ω . This can easily be done by changing $i\omega_n$ in Eq. (15) to ω . Consequently, the final expression for the self-energy reads

$$\Sigma_i^{\text{R,A}}(\mathbf{k}, \omega) = \int_0^\infty d\Omega \sum_{\mathbf{k}'} \delta(\epsilon_{\mathbf{k}'}) \alpha_i^2(\mathbf{k}, \mathbf{k}', \Omega) F(\Omega) L(\omega \pm i\delta, \Omega), \quad (16)$$

where

$$L(\omega \pm i\delta, \Omega) = \int_{-\infty}^\infty d\epsilon \left[\frac{N(\Omega) + 1 - f(\epsilon)}{\omega - \Omega - \epsilon \pm i\delta} + \frac{N(\Omega) + f(\epsilon)}{\omega + \Omega - \epsilon \pm i\delta} \right]. \quad (17)$$

The function $\Sigma_i^{\text{R(A)}}(\mathbf{k}, \omega)$ denotes the retarded (advanced) self-energy which is an analytical function of the variable ω in the upper (lower) half of the complex plane. The integral in (17) can be evaluated analytically, yielding

$$L(\omega, \Omega) = -2\pi i \left[N(\Omega) + \frac{1}{2} \right] + \Psi \left(\frac{1}{2} + i \frac{\Omega - \omega}{2\pi T} \right) - \Psi \left(\frac{1}{2} - i \frac{\Omega + \omega}{2\pi T} \right), \quad (18)$$

where $\Psi(z)$ is the digamma function. The self-energy $\Sigma_i^{\text{R,A}}(\mathbf{k}, \omega)$ expressed by Eq. (16) depends only on the direction of the momentum \mathbf{k} on the Fermi surface. It is convenient to present this dependence by expanding all functions involved in this expression over the complete and orthonormal set of functions introduced by Allen [14]. These so-called ‘‘Fermi surface harmonics’’, $\Psi_j(\mathbf{k})$, satisfy the condition

$$\sum_{\mathbf{k}} \Psi_j(\mathbf{k}) \Psi_{j'}(\mathbf{k}) \delta(\epsilon_{\mathbf{k}} - \epsilon) = \delta_{jj'} N(\epsilon) , \quad (19)$$

where

$$N(\epsilon) = \sum_{\mathbf{k}} \delta(\epsilon_{\mathbf{k}} - \epsilon) . \quad (20)$$

In terms of this set we write

$$\Sigma_i^{\text{R,A}}(\mathbf{k}, \omega) = \sum_j \Sigma_{i,j}^{\text{R,A}}(\omega) \Psi_j(\mathbf{k}) \quad (21)$$

$$G_i^{\text{R,A}}(\mathbf{k}, \omega) = \sum_j G_{i,j}^{\text{R,A}}(\epsilon_{\mathbf{k}}, \omega) \Psi_j(\mathbf{k}) \quad (22)$$

$$\begin{aligned} \alpha_{j,j'}^2(\mathbf{k}, \Omega) F(\Omega) &= \sum_{j,j'} \sum_{\mathbf{k}', \lambda} \delta(\epsilon_{\mathbf{k}'}) \left\{ |g_{\mathbf{k}'}(\mathbf{k} - \mathbf{k}', i, i', \lambda)|^2 \text{Im } D_\lambda(\mathbf{k} - \mathbf{k}', \omega) \right\}_{jj'} \times \\ &\times \Psi_j(\mathbf{k}) \Psi_{j'}(\mathbf{k}') . \end{aligned} \quad (23)$$

It follows from Eqs. (21-23) that the self-energy coefficients $\Sigma_{i,j}^{\text{R,A}}(\omega)$ are given by

$$\Sigma_{i,j}^{\text{R,A}}(\omega) = \sum_{j'} \int_0^\infty d\Omega \alpha_{j,j'}^2(\Omega) F(\Omega) L(\omega \pm i\delta, \Omega) , \quad (24)$$

where

$$\alpha_{j,j'}^2(\Omega) F(\Omega) = \frac{1}{N(0)} \sum_{\mathbf{k}} \sum_{\mathbf{k}'} \delta(\epsilon_{\mathbf{k}}) \delta(\epsilon_{\mathbf{k}'}) \alpha^2(\mathbf{k}, \mathbf{k}', \Omega) F(\Omega) \Psi_j(\mathbf{k}) \Psi_{j'}(\mathbf{k}') . \quad (25)$$

Here $N(0)$ denotes the density of electron states on the Fermi surface. The first Fermi harmonic is $\Psi_0(\mathbf{k}) = 1$ and the function

$$\alpha_{0,0}^2(\Omega) F(\Omega) = \frac{1}{N(0)} \sum_{\mathbf{k}} \sum_{\mathbf{k}'} \delta(\epsilon_{\mathbf{k}}) \delta(\epsilon_{\mathbf{k}'}) \alpha^2(\mathbf{k}, \mathbf{k}', \Omega) F(\Omega) \quad (26)$$

is obviously the well known Eliashberg spectral function which determines the superconductivity of metals in the simple s -pairing case. Introducing the real and imaginary parts of the self-energy, $\Sigma_1(\mathbf{k}, \omega)$ and $\Sigma_2(\mathbf{k}, \omega)$, respectively, the Green's function becomes

$$G^{-1}(\mathbf{k}, \omega + i\delta) = \omega - \epsilon_{\mathbf{k}} - \Sigma_1(\mathbf{k}, \omega + i\delta) - i\Sigma_2(\mathbf{k}, \omega + i\delta) . \quad (27)$$

The pole of the Green's function determines the spectrum of one-particle excitations. At small energies Eq. (27) can be rewritten as

$$G^{-1}(\mathbf{k}, \omega + i\delta) = \omega \left(1 - \frac{\partial \Sigma_1(\mathbf{k}, \omega)}{\partial \omega} \bigg|_{\omega=0} \right) - i\Sigma_2(\mathbf{k}, \omega + i\delta) . \quad (28)$$

Then the pole of G occurs at ω_0 , which is given by

$$\omega_0 = E_{\mathbf{k}} - \frac{i}{2\tau_{\mathbf{k}}} , \quad (29)$$

$$E_{\mathbf{k}} = \left(1 - \frac{\partial \Sigma_1(\mathbf{k}, \omega)}{\partial \omega}\right)^{-1} \epsilon_{\mathbf{k}} , \quad (30)$$

$$\frac{1}{2\tau_{\mathbf{k}}} = - \left(1 - \frac{\partial \Sigma_1(\mathbf{k}, \omega)}{\partial \omega}\right)^{-1} \Sigma_2(\mathbf{k}, E_{\mathbf{k}}) . \quad (31)$$

Here

$$\lambda_{\mathbf{k}} = - \left. \frac{\partial \Sigma_1(\mathbf{k}, \omega)}{\partial \omega} \right|_{\omega=0} \quad (32)$$

describes the change of the effective mass of the electron, while $\frac{1}{2\tau_{\mathbf{k}}}$ describes their relaxation rate. All functions can be rewritten in terms of Fermi harmonics and the spectral function $\alpha_{j,j'}^2(\Omega)F(\Omega)$. We shall turn to this problem later when we discuss the conductivity of metals in the presence of electron–phonon interaction.

As usual we write the conductivity of a metal in the presence of electron–phonon interaction in terms of the analytically continued electromagnetic kernel $K_{\alpha\beta}(\omega)$,

$$\sigma_{\alpha\beta}(\omega) = \frac{e^2 K_{\alpha\beta}(\omega)}{4\pi i \omega} , \quad (33)$$

which, in turn, is expressed through the one–particle Green’s function $G_i(\mathbf{k}, \omega)$ and corresponding vertex function Γ_{β} . In the framework of the thermodynamical theory of the perturbations the expression for $K_{\alpha\beta}(\omega)$ is

$$\begin{aligned} K_{\alpha\beta}(i\omega_n) = T \sum_{\omega_{n'}} \sum_{\mathbf{k}'} v_{\mathbf{k}'}^{\alpha} G(\mathbf{k}', i\omega_{n'}) G(\mathbf{k}', i\omega_{n'} + i\omega) \times \\ \times \Gamma_{\beta}(\mathbf{k}', i\omega_{n'}, i\omega_{n'} + i\omega) , \end{aligned} \quad (34)$$

where $v_{\mathbf{k}'}^{\alpha}$ is the α –component of the electron velocity. Using the ladder diagram approximation the equation for the vertex function is written as [1]

$$\begin{aligned} \Gamma_{\beta}(\mathbf{k}', i\omega_{n'}, i\omega_{n'} + i\omega_n) = v_{\mathbf{k}'}^{\beta} + T \sum_{\mathbf{k}'', n''} |\langle g_{\mathbf{k}''}(\mathbf{k}' - \mathbf{k}'', i, i', \lambda) \rangle|^2 \times \\ \times D_{\lambda}(\mathbf{k}' - \mathbf{k}'', i\omega_{n'} - i\omega_{n''}) G(\mathbf{k}'', i\omega_{n''}) G(\mathbf{k}'', i\omega_{n''} + i\omega_n) \times \\ \times \Gamma_{\beta}(\mathbf{k}'', i\omega_{n''}, i\omega_{n''} + i\omega_n) . \end{aligned} \quad (35)$$

Before we solve Eqs. (34) and (35) we simplify them somewhat. Firstly, as the conductivity of any metal in the absence of a magnetic field can be diagonalised in the appropriate representation we omit in the following the indices α and β considering the conductivity as a scalar. This is done bearing in mind that the absolute value of the conductivity in non–cubic crystals is anisotropic and that the corresponding functions determining the temperature and frequency dependence of $\sigma(\omega, T)$ reflect this anisotropy. Secondly, we omit the electron band indexes taking into account that interband transitions can be calculated separately if needed. We also omit the electron spin index multiplying by two the sum over the electron momentum \mathbf{k} . After that Eq. (35) is rewritten in a simplified form

$$\begin{aligned}
\Gamma_x(\mathbf{k}', i\omega_{n'}, i\omega_{n'} + i\omega_n) &= v_{\mathbf{k}'}^x + 2T \sum_{\mathbf{k}''} \sum_{n''} v_{\mathbf{k}''}^x \int_{-\infty}^{\infty} d\epsilon \delta(\epsilon - \epsilon_{\mathbf{k}''}) \times \\
&\times \frac{1}{\pi} \int_0^{\infty} d\Omega \alpha^2(\mathbf{k}', \mathbf{k}'') F(\Omega) \times \\
&\times \left(\frac{1}{i\omega_{n'} - i\omega_{n''} - \Omega} - \frac{1}{i\omega_{n'} - i\omega_{n''} + \Omega} \right) \times \\
&\times G(\mathbf{k}'', i\omega_{n''}) G(\mathbf{k}'', i\omega_{n''} + i\omega_n) \times \\
&\times \Gamma_x(\mathbf{k}'', i\omega_{n''}, i\omega_{n''} + i\omega_n) .
\end{aligned} \tag{36}$$

To establish some important steps in the derivation of the general formula for $\sigma(\omega)$ we consider, as a first step, the case where the vertex correction to the bare vertex $\Gamma_{\mathbf{k}}^x$ can be neglected. Then the expression for the electromagnetic response kernel $K(i\omega_n)$ becomes

$$\begin{aligned}
K_{xx}(i\omega_n) &= 2T \sum_{\mathbf{k}'} \sum_{\omega_{n'}=-\infty}^{\infty} \int d\epsilon \delta(\epsilon - \epsilon_{\mathbf{k}'}) (v_{\mathbf{k}'}^x)^2 \times \\
&\times G(\mathbf{k}', i\omega_{n'}) G(\mathbf{k}', i\omega_{n'} + i\omega_n) .
\end{aligned} \tag{37}$$

We can now use the Poisson summation formula

$$\sum_{n=-\infty}^{\infty} F(i\omega_n) = -\frac{1}{2\pi iT} \int_C d\omega \frac{F(\omega)}{e^{\frac{\omega}{T}} + 1} , \tag{38}$$

where the contour C encircles the imaginary ω -axis. After that we expand the ω -contour to infinity, picking up contributions from the singularities of our integrand at $i\omega_n = \epsilon_{\mathbf{k}'}$ and $i\omega_n = \epsilon_{\mathbf{k}'} - i\omega_n$. As a result we find after rather lengthy but simple calculation the analytically continued electromagnetic kernel as

$$\begin{aligned}
K(\omega) &= 2 \sum_{\mathbf{k}'} (v_{\mathbf{k}'}^x)^2 \int_{-\infty}^{\infty} d\epsilon \delta(\epsilon - \epsilon_{\mathbf{k}'}) \int_{-\infty}^{\infty} d\omega' \times \\
&\times \left(\tanh\left(\frac{\omega'}{2T}\right) - \tanh\left(\frac{\omega' + \omega}{2T}\right) \right) \times \\
&\times \Pi_0^{\text{RA}}(\mathbf{k}', \omega', \omega) .
\end{aligned} \tag{39}$$

Here $\Pi_0^{\text{RA}}(\mathbf{k}', \omega', \omega)$ has the form

$$\Pi_0^{\text{RA}}(\mathbf{k}', \omega', \omega) = G^{\text{R}}(\mathbf{k}', \omega' + \omega) G^{\text{A}}(\mathbf{k}', \omega') , \tag{40}$$

where $G^{\text{R}}(\mathbf{k}', \omega' + \omega)$ and $G^{\text{A}}(\mathbf{k}', \omega')$ are the retarded and advanced Green's function, respectively. Their self-energy parts are given by Eqs. (16 - 18). Just as in the case of the one-particle Green's function the relevant values of ω are small in comparison to the Fermi energy, the value of ϵ in $\delta(\epsilon - \epsilon_{\mathbf{k}})$ can be neglected, and the integration over ϵ can be carried out. As result we find for the conductivity

$$\sigma(\omega) = \frac{e^2}{4\pi i\omega} \sum_{\mathbf{k}} (v_{\mathbf{k}}^x)^2 \delta(\epsilon_{\mathbf{k}}) \int_{-\infty}^{\infty} d\omega' \left(\tanh\left(\frac{\omega' + \omega}{2T}\right) - \tanh\left(\frac{\omega'}{2T}\right) \right) \times \Pi_0(\hat{\mathbf{k}}_F, \omega', \omega), \quad (41)$$

where the function $\Pi_0(\hat{\mathbf{k}}_F, \omega', \omega)$ depends on the position of the momentum $\hat{\mathbf{k}}_F$ on the Fermi surface and is given by

$$\Pi_0(\hat{\mathbf{k}}_F, \omega', \omega) = \frac{1}{\omega + \Sigma^R(\hat{\mathbf{k}}_F, \omega + \omega') - \Sigma^A(\hat{\mathbf{k}}_F, \omega')}. \quad (42)$$

For the quasi-isotropic case we get, of course, the well known result for the optical conductivity [14,15]

$$\sigma(\omega) = \frac{\omega_{\text{pl}}^2}{4\pi i\omega} \int_{-\infty}^{\infty} d\omega' \left(\tanh\left(\frac{\omega' + \omega}{2T}\right) - \tanh\left(\frac{\omega'}{2T}\right) \right) \Pi_0(\omega, \omega'), \quad (43)$$

where the plasma frequency of electrons ω_{pl} is

$$\omega_{\text{pl}}^2 = 2e^2 \sum_{\mathbf{k}} (v_{\mathbf{k}}^x)^2 \delta(\epsilon_{\mathbf{k}}) \quad (44)$$

and the function $\Pi_0(\omega, \omega')$ is

$$\Pi_0(\omega, \omega') = \frac{1}{\omega + \Sigma^R(\omega + \omega') - \Sigma^A(\omega') + \frac{i}{\tau_{\text{imp}}}}. \quad (45)$$

Here we introduced the relaxation rate from impurity scattering $\frac{1}{\tau_{\text{imp}}}$.

For the anisotropic case we should expand all functions under the integral in Eq. (41) over the Fermi harmonics. The value $(v_{\mathbf{k}}^x)^2$ is just the square of the Fermi harmonic of the order $N = 1$ (for details see Ref. [14]). The expansion of the function $\Pi_0(\hat{\mathbf{k}}_F, \omega', \omega)$ can be written as

$$\Pi_0(\hat{\mathbf{k}}_F, \omega', \omega) = \sum_j \Pi_j(\omega', \omega) F_j(\hat{\mathbf{k}}_F). \quad (46)$$

The non-zero result for the conductivity will arise from the first harmonic, $F_j(\hat{\mathbf{k}}_F) = 1$, and from the harmonics with even order $N \geq 2$. The first harmonic gives the same result as found for the isotropic case. An example of a higher harmonic is the one which transforms as the representation Γ_{12} of the crystal symmetry. It has the form

$$\Psi_j^{\Gamma_{12}} = \frac{v_{yx}^2 - v_{xy}^2}{\langle (v_x^2 - v_y^2)^2 \rangle^{1/2}}. \quad (47)$$

At this point we are not certain to which extent the higher harmonics are relevant in HTSC systems but it is known that their influence is small in normal metals. This question should be considered in more detail but is beyond the scope of this paper.

While the analytic continuation of Eqs. (33), (34) in the zero-order approximation and absence of the vertex function $\Gamma(\mathbf{k}, i\omega_n, i\omega_m)$ is straightforward, it becomes a non-trivial task in the presence of $\Gamma(\mathbf{k}, i\omega_n, i\omega_m)$. The difficulty arises from the existence of a manifold of functions which can be obtained as a result of analytical continuation for one variable while another is fixed. However, this difficulty can be avoided by changing, as above, the sum over the Matsubara frequencies to a contour integral. The contour consists of (three) circuits around the imaginary axis of the variable ω' , avoiding all poles and branch cuts of the integrand. Using the methods developed in Refs. [1,16] we obtain

$$\sigma(\omega) = \frac{2}{4\pi i \omega} \sum_{\mathbf{k}} \int_{-\infty}^{\infty} d\epsilon \delta(\epsilon - \epsilon_{\mathbf{k}}) v_{\mathbf{k}}^x \int_{-\infty}^{\infty} \frac{d\omega'}{2\pi i} \left(\tanh\left(\frac{\omega' + \omega}{2T}\right) - \tanh\left(\frac{\omega'}{2T}\right) \right) \times \quad (48)$$

$$\times \Pi_0^{\text{RA}}(\mathbf{k}, \omega', \omega) \Gamma_x(\mathbf{k}, \omega', \omega)$$

and

$$\Gamma_x(\mathbf{k}, \omega', \omega) = v_{\mathbf{k}}^x + 2 \sum_{\mathbf{k}'} \int_{-\infty}^{\infty} d\epsilon \delta(\epsilon - \epsilon_{\mathbf{k}'}) \int_{-\infty}^{\infty} \frac{d\omega''}{2\pi i} \times \quad (49)$$

$$\times \left[\tanh\left(\frac{\omega'' + \omega}{2T}\right) \lambda_{\mathbf{k}\mathbf{k}'}(\omega' - \omega'' + i\delta) - \tanh\left(\frac{\omega''}{2T}\right) \lambda_{\mathbf{k}\mathbf{k}'}(\omega'' - \omega' - i\delta) + \right.$$

$$\left. + \coth\left(\frac{\omega' - \omega''}{2T}\right) (\lambda_{\mathbf{k}\mathbf{k}'}(\omega'' - \omega' + i\delta) - \lambda_{\mathbf{k}\mathbf{k}'}(\omega' - \omega'' - i\delta)) \right] \times$$

$$\times \Pi_0^{\text{RA}}(\mathbf{k}', \omega'', \omega) \Gamma_x(\mathbf{k}', \omega'', \omega) ,$$

where the function

$$\lambda_{\mathbf{k}\mathbf{k}'}(\omega) = \int_0^{\infty} d\Omega \alpha^2(\mathbf{k}, \mathbf{k}', \Omega) F(\Omega) \left[\frac{1}{\omega - \Omega} - \frac{1}{\omega + \Omega} \right] \quad (50)$$

was introduced. Taking into account that apart from $\Pi_0(\mathbf{k}', \omega'', \omega)$ all functions under the integral on the right-hand side of Eq. (49) depend only weakly on the variable $\epsilon_{\mathbf{k}'}$ we can integrate over this variable and find

$$\Gamma_x(\hat{\mathbf{k}}_{\text{F}}, \omega', \omega) = v_{\mathbf{k}}^x + \sum_{\mathbf{k}'} \delta(\epsilon_{\mathbf{k}'}) \int_{-\infty}^{\infty} d\omega'' \Pi_0(\hat{\mathbf{k}}'_{\text{F}}, \omega'', \omega) \times \quad (51)$$

$$\times [I(\omega' - i\delta, \Omega, \omega'') - I(\omega' + \omega + i\delta, \Omega, \omega'')] \Gamma_x(\hat{\mathbf{k}}'_{\text{F}}, \omega'', \omega) .$$

Here $\Pi_0(\hat{\mathbf{k}}'_{\text{F}}, \omega'', \omega)$ is defined by Eq. (42) and $I(\omega, \Omega, \omega')$ is

$$I(\omega, \Omega, \omega') = \frac{1 - f(\omega') + N(\Omega)}{\omega - \Omega - \omega'} + \frac{f(\omega') + N(\Omega)}{\omega + \Omega - \omega'} . \quad (52)$$

At this stage it is useful to introduce a new function $\gamma_x(\hat{\mathbf{k}}_{\text{F}}, \omega', \omega)$,

$$\gamma_x(\hat{\mathbf{k}}_{\text{F}}, \omega', \omega) = \Pi_0(\hat{\mathbf{k}}_{\text{F}}, \omega', \omega) \Gamma_x(\hat{\mathbf{k}}_{\text{F}}, \omega', \omega) . \quad (53)$$

In terms of this function the conductivity can be expressed as

$$\sigma(\omega) = \frac{2}{4\pi i \omega} \sum_{\mathbf{k}} \delta(\epsilon_{\mathbf{k}}) v_{\mathbf{k}}^x \int_{-\infty}^{\infty} d\omega' \left(\tanh\left(\frac{\omega' + \omega}{2T}\right) - \tanh\left(\frac{\omega'}{2T}\right) \right) \times \gamma_x(\hat{\mathbf{k}}_{\mathbf{F}}, \omega', \omega). \quad (54)$$

For $\gamma_x(\hat{\mathbf{k}}_{\mathbf{F}}, \omega', \omega)$ one can write the equation

$$\begin{aligned} \omega \gamma_x(\hat{\mathbf{k}}_{\mathbf{F}}, \omega', \omega) &= v_{\mathbf{k}}^x + \sum_{\mathbf{k}'} \delta(\epsilon_{\mathbf{k}'}) \int_0^{\infty} d\Omega \alpha^2(\mathbf{k}, \mathbf{k}', \Omega) F(\Omega) \times \\ &\times \int_{-\infty}^{\infty} d\omega'' [I(\omega' - i\delta, \Omega, \omega'') - I(\omega' + \omega + i\delta, \Omega, \omega'')] \times \\ &\times (\gamma_x(\hat{\mathbf{k}}'_{\mathbf{F}}, \omega'', \omega) - \gamma_x(\hat{\mathbf{k}}_{\mathbf{F}}, \omega', \omega)). \end{aligned} \quad (55)$$

Now we use the expansion of the functions in Eq. (55) in Fermi harmonics. This yields

$$\begin{aligned} \omega \gamma_j(\omega', \omega) &= \langle v_x^2 \rangle^{1/2} \delta_{jx} + \sum_{j'} \int_0^{\infty} d\Omega \times \\ &\times \int_{-\infty}^{\infty} d\omega'' [I(\omega' - i\delta, \Omega, \omega'') - I(\omega' + \omega + i\delta, \Omega, \omega'')] \times \\ &\times \left(\alpha_{jj'}^2(\Omega) F(\Omega) \gamma_{j'}(\omega'', \omega) - \sum_{j''} C_{jj'j''} \alpha_{j''0}^2(\Omega) F(\Omega) \gamma_{j'}(\omega'', \omega) \right), \end{aligned} \quad (56)$$

where we used the Clebsh–Gordon coefficients

$$C_{jj'j''} = \frac{1}{N(0)} \sum_{\mathbf{k}} \delta(\epsilon_{\mathbf{k}}) \Psi_j(\mathbf{k}) \Psi_{j'}(\mathbf{k}) \Psi_{j''}(\mathbf{k}). \quad (57)$$

All following calculations are greatly simplified if

$$\alpha_{jj'}^2(\Omega) F(\Omega) = \frac{1}{N(0)} \sum_{\mathbf{k}} \sum_{\mathbf{k}'} \delta(\epsilon_{\mathbf{k}}) \delta(\epsilon_{\mathbf{k}'}) \alpha^2(\mathbf{k}, \mathbf{k}', \Omega) F(\Omega) \Psi_j(\mathbf{k}) \Psi_{j'}(\mathbf{k}') \quad (58)$$

has the diagonal form

$$\alpha_{jj'}^2(\Omega) F(\Omega) = \alpha_j^2(\Omega) F(\Omega) \delta_{jj'}. \quad (59)$$

In ordinary metals this assumption is well satisfied, where $\alpha^2(\mathbf{k}, \mathbf{k}', \Omega) F(\Omega)$ depends mainly on the difference of the momenta $\mathbf{k} - \mathbf{k}'$. There are also some restrictions on the non-diagonal matrix elements $\alpha_{jj'}^2(\Omega) F(\Omega)$, $j \neq j'$, connected with the crystal symmetries (see e. g. Ref. [14]). Nevertheless, it is difficult to say something definite about the accuracy of this assumption in HTSC systems without concrete calculations of the functions $\alpha^2(\mathbf{k}, \mathbf{k}', \Omega) F(\Omega)$. Such calculations were never made until now. We use this approximation as a first step. In addition, we restrict ourself to the use of the first two Fermi harmonics.

It is useful to search for the solution of Eq. (56) in the form

$$\gamma_1(\omega' \omega) = \frac{1}{\omega + \Sigma_{\text{tr}}^{\text{R}}(\omega' + \omega, \omega') - \Sigma_{\text{tr}}^{\text{A}}(\omega', \omega)} , \quad (60)$$

where, after lengthy but simple calculations, the equations for the transport “self-energies” can be written in the form

$$\begin{aligned} \Sigma_{\text{tr}}^{\text{R}}(\omega' + \omega, \omega') &= \frac{1}{N(0)} \sum_{\mathbf{k}} \sum_{\mathbf{k}', \lambda} \int_0^\infty d\Omega \int_{-\infty}^\infty d\omega'' I(\omega' + \omega + i\delta, \Omega, \omega'') |g_{\mathbf{k}}(\mathbf{k}' - \mathbf{k}, \lambda)|^2 \times \\ &\times \text{Im} D_\lambda(\mathbf{k} - \mathbf{k}', \omega') \frac{v_x^2}{\langle v_x^2 \rangle} \left(1 - \frac{v'_x}{v_x} \frac{\omega + \Sigma_{\text{tr}}^{\text{R}}(\omega' + \omega, \omega') - \Sigma_{\text{tr}}^{\text{A}}(\omega', \omega)}{\omega + \Sigma_{\text{tr}}^{\text{R}}(\omega'' + \omega, \omega') - \Sigma_{\text{tr}}^{\text{A}}(\omega'', \omega')} \right) \end{aligned} \quad (61)$$

and

$$\begin{aligned} \Sigma_{\text{tr}}^{\text{A}}(\omega', \omega) &= \frac{1}{N(0)} \sum_{\mathbf{k}} \sum_{\mathbf{k}', \lambda} \int_0^\infty d\Omega \int_{-\infty}^\infty d\omega'' I(\omega' - i\delta, \Omega, \omega'') |g_{\mathbf{k}}^2(\mathbf{k}' - \mathbf{k}, \lambda)| \times \\ &\times \text{Im} D_\lambda(\mathbf{k} - \mathbf{k}', \omega') \frac{v_x^2}{\langle v_x^2 \rangle} \left(1 - \frac{v'_x}{v_x} \frac{\omega + \Sigma_{\text{tr}}^{\text{R}}(\omega' + \omega, \omega') - \Sigma_{\text{tr}}^{\text{A}}(\omega', \omega)}{\omega + \Sigma_{\text{tr}}^{\text{R}}(\omega'' + \omega, \omega') - \Sigma_{\text{tr}}^{\text{A}}(\omega'', \omega')} \right) . \end{aligned} \quad (62)$$

The Eqs. (61) and (62) are still implicitly integral equations for $\Sigma_{\text{tr}}^{\text{R,A}}$. However, the integrand on the right hand side of Eqs. (61) and (62) depends only weakly on the functions $\Sigma_{\text{tr}}^{\text{R,A}}$. The detailed numerical analysis of these equations, given by Allen [2] for the case $T = 0$, has shown that the assumption

$$\frac{\omega - \Sigma_{\text{tr}}^{\text{R}}(\omega' + \omega, \omega') - \Sigma_{\text{tr}}^{\text{A}}(\omega', \omega)}{\omega - \Sigma_{\text{tr}}^{\text{R}}(\omega'' + \omega, \omega') - \Sigma_{\text{tr}}^{\text{A}}(\omega'', \omega')} = 1 \quad (63)$$

is satisfied with good accuracy. The only difference in Eq. (61) compared to Eqs. (43) and (45) is the appearance of the transport “self-energies” $\Sigma_{\text{tr}}^{\text{R,A}}$ instead of the one-particle self-energies. Accordingly, the equations for $\Sigma_{\text{tr}}^{\text{R,A}}$ can be written in a form which largely resembles the equations for the one-particle self-energies, namely

$$\Sigma_{\text{tr}}^{\text{R}}(\omega' + \omega, \omega) = \int_0^\infty d\Omega \alpha_{\text{tr}}^2(\Omega) F(\Omega) \int_{-\infty}^\infty d\omega'' I(\omega' + \omega + i\delta, \Omega, \omega'') , \quad (64)$$

$$\Sigma_{\text{tr}}^{\text{A}}(\omega', \omega) = \int_0^\infty d\Omega \alpha_{\text{tr}}^2(\Omega) F(\Omega) \int_{-\infty}^\infty d\omega'' I(\omega' - i\delta, \Omega, \omega'') , \quad (65)$$

and

$$\begin{aligned} \alpha_{\text{tr}}^2(\Omega) F(\Omega) &= \frac{1}{N(0)} \sum_{\mathbf{k}} \sum_{\mathbf{k}', \lambda} \delta(\epsilon_{\mathbf{k}}) \delta(\epsilon_{\mathbf{k}'}) \int_{-\infty}^\infty d\omega'' |g_{\mathbf{k}}^2(\mathbf{k} - \mathbf{k}', \lambda)|^2 \text{Im} D_\lambda(\Omega) \times \\ &\times \frac{v_{\mathbf{k}}^2}{\langle v_{\mathbf{k}}^2 \rangle} \left(1 - \frac{v_{\mathbf{k}'}}{v_{\mathbf{k}}} \right) . \end{aligned} \quad (66)$$

The expression for the conductivity can then be written in a form which is formally identical to Eq. (43) obtained without vertex corrections

$$\sigma(\omega) = \frac{\omega_{\text{pl}}^2}{4\pi i\omega} \int_{-\infty}^{\infty} d\omega' \left(\tanh\left(\frac{\omega' + \omega}{2T}\right) - \tanh\left(\frac{\omega'}{2T}\right) \right) \times \frac{1}{\omega + \Sigma_{\text{tr}}^{\text{R}}(\omega' + \omega) - \Sigma_{\text{tr}}^{\text{A}}(\omega' + \omega) + \frac{i}{\tau_{\text{imp}}}} . \quad (67)$$

Equation (67) has just the form which is normally used for the calculation of the transport properties of metals (see. e. g. [10,14]).

The expression (67) for the conductivity can be simplified even more in the case of weak electron-phonon interaction [7], to yield the so-called “extended” Drude formula

$$\sigma(\omega) = \frac{\omega_{\text{pl}}^2}{4\pi} \frac{1}{i\omega - W(\omega) - \frac{1}{\tau_{\text{imp}}}} , \quad (68)$$

where

$$W(\omega) = i\omega \left(1 - \frac{m_{\text{tr}}^*(\omega)}{m} \right) + \frac{1}{\tau_{\text{tr}}(\omega)} , \quad (69)$$

$$W(\omega) = -2i \int_0^{\infty} d\Omega \alpha_{\text{tr}}^2(\Omega) F(\Omega) K\left(\frac{\omega}{2\pi T}, \frac{\Omega}{2\pi T}\right) , \quad (70)$$

and the function $K\left(\frac{\omega}{2\pi T}, \frac{\Omega}{2\pi T}\right)$ has the form

$$K(x, y) = \frac{i}{y} + \left\{ \frac{y-x}{x} [\Psi(1-ix+iy) - \Psi(1+iy)] \right\} - \{y \longleftrightarrow -y\} . \quad (71)$$

Firstly, we shall check the accuracy of the approximation of the expression (67) for $\sigma(\omega)$ by the “extended” Drude formula, Eq. (68). For that purpose we use the transport spectral function $\alpha_{\text{tr}}^2(\omega)F(\omega)$ of the form shown in Fig. 1. A comparison between Eqs. (67) and (68) is shown in Fig. 2 for constants of coupling $\lambda_{\text{tr}} = 1$, where

$$\lambda_{\text{tr}} = 2 \int_0^{\infty} \frac{d\Omega}{\Omega} \alpha_{\text{tr}}^2(\Omega) F(\Omega) . \quad (72)$$

There are some differences in the low energy regime, $\omega \lesssim 200 \text{ cm}^{-1}$, shown in Fig. 3, especially at low temperatures. One should be careful using the “extended” Drude formula in this case. However, even in this region the difference is rather small. The difference between the conductivity calculated by the formulae (67) and (68) continues to be small even for a constant of coupling $\lambda \simeq 2$.

The transport relaxation rate

$$\frac{1}{\tau_{\text{tr}}^*(\omega)} = \frac{1}{\tau_{\text{tr}}(\omega)} \frac{m}{m^*(\omega)} \quad (73)$$

has a universal behaviour for metals with different values of λ and different phonon density of states. Figure 4 shows the frequency dependence of the relaxation rate $\frac{1}{\tau_{\text{tr}}(\omega)}$ in dimensionless form. Here ω_m is the value of the maximum phonon frequency (i. e. the end of the phonon spectrum). The six different curves plotted in Fig. 4 are indistinguishable as function of the dimensionless energy ω/ω_m . The quantity $\frac{1}{\tau_{\text{tr}}^*(\omega)}$ is also rather universal as a function of the dimensionless temperature $T/\pi\omega_m$. Figure 5 shows $\frac{1}{\tau_{\text{tr}}^*(\omega)}$ for $T = 10$ K and 100 K. Firstly, we would like to emphasise the quasi-linear ω -dependence of $\frac{1}{\tau_{\text{tr}}^*(\omega)}$ over a large energy interval, $0.5 \leq \omega \leq (3-4)\omega_m$. The function $\frac{1}{\tau_{\text{tr}}^*(\omega)}$ increases with increasing energy ω up to very high values, $\omega \simeq 10\omega_m$. This contrasts strongly with the behaviour of the one-particle relaxation rate $\frac{1}{\tau(\omega)}$ defined by Eq. (31) and shown in the inset of Fig. 5. It is well known [17] that the latter rapidly increases with energy and becomes constant for $\omega \geq \omega_m$. This difference in the behaviour of the functions $\frac{1}{\tau_{\text{tr}}^*(\omega)}$ and $\frac{1}{\tau(\omega)}$ was first discussed in Ref. [6].

As mentioned above, there are only a few investigations [4,5] of the influence of the electron-phonon interaction on the optical spectra of normal state metals where the frequency dependence of these effects was observed. Besides the reasons mentioned above there is another very important reason for the small number of such investigations. Namely, the absolute values of the frequency dependence of the discussed effects is determined by the value of $\frac{1}{\tau_{\text{tr}}^*(\omega)}$ at $\omega \rightarrow \infty$ [6]. This function can be written as

$$\lim_{\omega \rightarrow \infty} \frac{1}{\tau_{\text{tr}}^*(\omega)} = \pi \lambda \langle \omega \rangle , \quad (74)$$

where

$$\lambda \langle \omega \rangle = 2 \int_0^\infty d\omega \alpha_{\text{tr}}^2(\omega) F(\omega) . \quad (75)$$

This value can be expressed as

$$\frac{1}{\tau_{\text{tr}}^*} \simeq (1-2) \lambda \omega_m , \quad (76)$$

as can be seen from Figs. 4 and 5, and it is very small for ordinary metals. In lead, for example, one finds $\lambda \langle \omega \rangle \approx 100 \text{ cm}^{-1}$. It is extremely difficult to observe this phenomena in the usual reflection spectra. Therefore, the observation of Holstein processes in lead was made [4,5] using the light scattering inside a cavity whose walls hold the sample material. It was averaged over at least 100 such reflections to increase the accuracy of the experiment. It was shown [7,18] that a far-infrared measurement at low temperature, containing phonon-induced structure, can be inverted to give the spectral function of the electron-phonon interaction $\alpha_{\text{tr}}^2(\omega)F(\omega)$. This function was obtained in Ref. [18] for lead in very good agreement with experimental data from tunnelling measurements. We shall come back to discuss this observation in some more detail.

III. ELECTRON-PHONON INTERACTION AND OPTICAL SPECTRA OF HTSC SYSTEMS

A large amount of work has been devoted to the study of optical spectra of HTSC systems (see for example the reviews [19,20]). Investigations include normal and superconducting

state properties, doping dependence, the effect of impurities, etc.. Here, we shall restrict our analysis to optimally doped HTSC in the normal state. In this case the optical spectra of all HTSC materials show quite similar behaviour: their reflectivity drops nearly linearly with energy from $R \simeq 1$ down to $R \simeq 0.1$ at the plasma edge ω_p^* , where the values of ω_p^* vary for different HTSC materials, $1 \text{ eV} \leq \omega_p^* \leq 1.8 \text{ eV}$ [20]. Measurements for different HTSC compounds further coincide in showing large values for the conductivity in the energy interval $2 \text{ eV} < \omega < 15 \text{ eV}$ and well developed charge fluctuation spectra (described by the energy loss function $-\text{Im}(\frac{1}{\epsilon(\omega)})$) in the energy interval $5 \text{ eV} < \omega < 40 \text{ eV}$ [21]. The high energy part of spectra above a few eV can be well described in terms of the usual band structure calculations [20,22]. Moreover, the calculations [22,23] can also describe quite accurately some low energy interband transitions in $\text{YBa}_2\text{Cu}_3\text{O}_7$ [24].

The most unusual part of the optical spectra of HTSC systems is connected with the strong decrease in reflectivity, almost linear in energy, in the region $0 \leq \omega \leq \omega_p^* \simeq 1 \text{ eV}$ [25]. This behaviour certainly cannot be explained with the simple Drude approach. Thomas *et al* [26] proposed two different ways of analysing such spectra. First, a one-component Fermi-liquid approach, using the “extended” Drude formula with frequency dependent mass $m^*(\omega)$ and relaxation rate $\frac{1}{\tau(\omega)}$. This model successfully describes the heavy fermion systems [27]. Secondly, a two-component approach, where the spectrum is decomposed in two components, the Drude part and a mid-infrared (MIR) absorption band. In the latter case there is no unique way of separating the two components.

As we have discussed above, including the electron-phonon interaction in the consideration leads immediately to the representation of the optical conductivity in terms of the “extended” Drude formula. It has been shown earlier for some HTSC [6,8] that the existence of strong electron-phonon coupling, including some amount of MIR excitations, can indeed explain their optical conductivity. We now consider this approach in some more detail. To describe the optical spectra of HTSC systems we use the formulae obtained in section II using a transport spectral function $\alpha_{\text{tr}}^2(\omega)F(\omega)$ of the form shown in Fig. 1, multiplied by ω^2 . This spectral function extends up to $\omega_m = 735 \text{ cm}^{-1}$ and well resembles the phonon spectra of HTSC systems. Generally, the optical properties do not depend on the actual shape of $\alpha_{\text{tr}}^2(\omega)F(\omega)$ but on some moments of it. Thus, we use the constant of electron-phonon coupling λ_{tr} as defined in Eq. (72) as fit parameter.

Figure 6 shows the reflectivity of optimally doped $\text{La}_{2-x}\text{Sr}_x\text{CuO}_4$ (LSCO) at room temperature. We have used the values $\omega_p = 1.8 \text{ eV}$ and $\epsilon_\infty = 4.6$ obtained by one of us [28] from band structure calculations. The contribution of the electron-phonon coupling was supposed to be $\lambda_{\text{tr}} = 2.5$. The resulting reflectivity corresponds well to measurements on good quality films [25]. The conductivity calculated in Ref. [28] describes well the optical spectra of LSCO at energies above $\approx 3 \text{ eV}$, as was confirmed by experiment [29]. Taking all this into account, we can conclude that the band structure approach joined with strong electron-phonon interaction can explain the overall behaviour of the optical spectrum of LSCO in the energy range $0 < \omega \leq 40 \text{ eV}$. Moreover, this approach also explains the temperature dependence of the optical spectrum of LSCO quite well. Figure 7 shows the reflectivity of LSCO in the FIR at temperatures $T = 100, 200, 300 \text{ K}$. The agreement between experimental [30] and calculated curves is good considering that the only fit parameter used was the constant of coupling λ_{tr} . In Fig. 8 we show the reflectivity for LSCO up to $\omega \approx 1 \text{ eV}$ for the same temperatures. The agreement between calculated and measured curves is still quite good on

this larger energy scale. Nevertheless, we should point out a small discrepancy in the MIR region. While this discrepancy is very small at $T = 100$ K, it becomes more pronounced with increasing temperature. Introducing a MIR band, this can be seen as further evidence for the temperature dependence of such a band, as discussed in Ref. [8].

We now focus on the temperature dependence of the optical reflectivity in $\text{YBa}_2\text{Cu}_3\text{O}_{7-\delta}$ (YBCO), using the values $\omega_p = 3$ eV and $\epsilon_\infty = 5.8$ obtained from band structure calculations [22]. Figure 9 shows the reflectivity of YBCO from Ref. [31] compared to our calculations for $T = 100, 200, 300$ K, where we have used an impurity scattering rate $\frac{1}{\tau_{\text{imp}}} = 300$ cm^{-1} in our calculation of the relaxation rate. The agreement between experimental and theoretical curves seems to be again quite good. The only fit parameter used here was $\lambda_{\text{tr}} = 3$. Certainly, there are some discrepancies between data and theoretical curves in Fig. 9. We should point out that discrepancies of nearly the same order exist between different type of monocrystals and films. Also, our approach is based on the quasi-isotropic approximation for the electron-phonon interaction which is clearly an oversimplification in these quasi-two dimensional systems. The inset of Fig. 9 shows the calculated reflectivity of YBCO up to 1.8 eV at room temperature. It can be seen that there is an upturn in the reflectivity at MIR frequencies which is certainly much larger than in LSCO. This confirms the observation made in Ref. [32] that the MIR band is more pronounced in YBCO than in LSCO. Furthermore, we know from band structure calculations [22] that YBCO systems show interband transitions with rather strong intensity in the MIR region.

Figure 10 shows the behaviour of the transport relaxation rate $\frac{1}{\tau_{\text{tr}}^*(\omega)}$ obtained for YBCO at temperatures $T = 100, 200, 300$ K. It well resembles the usual shape of such curves in HTSC and might be compared to Fig. 2 in Ref. [33], where the relaxation rate for $\text{Bi}_2\text{Sr}_2\text{CaCu}_2\text{O}_8$ was derived from the conductivity using the “extended” Drude formula. It was also shown there that the behaviour of the relaxation rate $\frac{1}{\tau_{\text{tr}}^*(\omega)}$ cannot be explained in the framework of marginal Fermi liquid theory [34], since $\frac{1}{\tau_{\text{tr}}^*(\omega)}$ saturates at energies $\omega > \omega_c \simeq 1500$ cm^{-1} whereas according to marginal Fermi liquid theory the relaxation rate should continue in a straight line. This argument was used in Ref. [33] as evidence against the one-component approach to the optical spectra of HTSC systems. However, the saturating behaviour for $\frac{1}{\tau_{\text{tr}}^*(\omega)}$ can be clearly seen in Fig. 10, at nearly the same energy as it was observed in $\text{Bi}_2\text{Sr}_2\text{CaCu}_2\text{O}_8$. Figure 11 shows the calculated resistivity for YBCO, demonstrating clearly a linear temperature dependence over a large temperature interval.

To conclude this considerations, we would like to discuss shortly the possibility of inverting reflectivity data to obtain the transport spectral function $\alpha_{\text{tr}}^2(\omega)F(\omega)$. This has been done for lead at $T = 0$ [18], where the the infrared data was obtained by applying a magnetic field to drive the system into the normal state. There, a spectral function with detailed structure could be obtained. In HTSC systems the situation is more complex. The superconducting state exists up to considerably high temperatures $T > T_c$ and cannot be suppressed by magnetic fields to allow IR measurements at $T = 0$. At finite temperature the inversion procedure is far more difficult and as a result such calculations only yield the rough overall form of the transport spectral function. Nevertheless, the resulting $\alpha_{\text{tr}}^2(\omega)F(\omega)$ clearly resemble the phonon spectra of these systems [7].

IV. CONCLUSION

The results obtained in this work demonstrate clearly, that strong electron–phonon interaction, combined with band structure calculations, describe the overall behaviour of the optical spectra and the main part of the transport properties of HTSC in a straightforward manner. However, we do not claim that this simple quasi–isotropic approach can explain all details of the behaviour of HTSC systems, even in the normal state, and even at optimal doping. There are a number of open problems concerning the behaviour of the Hall coefficient, the NMR relaxation rate of the copper sites. We would like to point out the existence of at least two relaxation rates in the HTSC systems, namely the quasi–particle relaxation rate $\frac{1}{\tau(\omega)}$ and the transport $\frac{1}{\tau_{tr}^*(\omega)}$ which are very different over a large energy range. We cannot rule out that the relaxation rate involved in the Hall current, due to strong and possibly anisotropic electron–phonon interaction, will be different from the transport relaxation rate in those systems. This could lead to the observed temperature dependence of the Hall coefficient.

Last but not least, we should point out that the simple approach presented here does not work at low temperatures. It cannot properly describe the anisotropy of the superconducting order parameter, although it yields the correct order of magnitude for the value of T_c . There are additional phenomena besides electron–phonon coupling which become important at low temperatures. There are a number of different models which combine a strong electron–phonon interaction with interband Coulomb interaction, with the existence of a Van Hove singularity in the electron spectrum, etc., of which a detailed discussion is beyond the scope of this work.

ACKNOWLEDGEMENT

The authors would like to thank O. Dolgov for many helpful discussions. They are also grateful to S. Shulga for providing his program for this calculations. E. G. M. would like to thank the Royal Society and the Department of Earth Sciences, University of Cambridge, for their support and kind hospitality during his visit to Cambridge. He also acknowledges the RFBI for the financial support during the early stages of this work.

REFERENCES

- [1] T. Holstein, *Ann. Phys. (N. Y.)* **29**, 410, (1969)
- [2] P. B. Allen, *Phys. Rev. B* **3**, 305 (1971)
- [3] G. B. Motulevich *Sov. Phys. Uspekhi*
- [4] R. R. Joyce and P. L. Richards, *Phys. Rev. Lett.* **24**, 1007 (1970)
- [5] J. G. Bednorz and K. A. Müller, *Z. Phys. B* **64**, 189 (1986)
- [6] S. V. Shulga, O. V. Dolgov, E. G. Maksimov, *Physica C* **178**, 226 (1991)
- [7] O. V. Dolgov, S. V. Shulga, *J. Supercond.* **6**, 611 (1995)
- [8] O. V. Dolgov, H. J. Kaufmann, E. K. H. Salje, and Y. Yagil *Physica C* **279**, 113 (1997)
- [9] P. B. Allen, in *Dynamical Properties of Solids*, G. K. Horton, A. A. Maradudin, eds. (Amsterdam, North Holland, 1980), Vol. 3, pp. 95
- [10] E. G. Maksimov, D. Yu Savrasov, and S. Yu Savrasov, *Physics — Uspekhi* **40**, 337 (1997)
- [11] D. Rainer, in *Progress in Low-Temperature Physics*, D. F. Brewer, eds. (Amsterdam, Elsevier, 1986), pp. 371
- [12] A. A. Abrikosov, L. P. Gor'kov, and I. E. Dzyaloshinski, *Methods of Quantum Field Theory in Statistical Physics*, (Dover, New York, 1963)
- [13] A. B. Migdal, *Sov. Phys. — JETP* **39**, 996 (1958)
- [14] P. B. Allen, *Phys. Rev. B* **13**, 1416 (1976)
- [15] W. Lee, D. Rainer, and W. Zimmerman, *Physica C* **159**, 535 (1989)
- [16] G. M. Eliashberg, *Sov. Phys. — JETP* **41**, 1241 (1961)
- [17] P. B. Allen, B. Mitrovich, in *Solid State Physics*, M. Ehrenreich, F. Seitz, D. Turnbull, eds. (Academic Press, New York, 1982) Vol. 37
- [18] B. Farworth, T. Timusk, *Phys. Rev. B* **14**, 5115 (1976)
- [19] D. B. Tanner, T. Timusk, in *Properties of High Temperature Superconductors*, D. M. Ginsberg, ed. (World Scientific, Singapore, 1992) Vol. 3, pp. 363
- [20] S. Tajima, *Superconductivity Review* **2**, 125 (1997)
- [21] N. Nücker, J. Fink, B. Renker, D. Everet, C. Politis, D. J. W. Weis, J. C. Fuggle, *Z. Phys. B* **67**, 9 (1987)
- [22] E. G. Maksimov, S. N. Rashkeev, S. Yu Savrasov, and Y. A. Uspenskii, *Phys. rev. Lett.* **13**, 1880 (1989); *Sov. Phys. — JETP* **70**, 952 (1990)
- [23] I. I. Mazin, D. Jepsen, O. K. Anderson, A. I. Leichtenstein, S. N. Reshkeev, Y. A. Uspenskii, *Phys. Rev. B* **45**, 5103 (1992)
- [24] B. Bucher, J. Karpinski, E. Kaldis, P. Wachter, *Phys. Rev. B* **45**, 3026 (1992)
- [25] I. Bozovic, J. H. Klein, J. J. Harris Jr. E. S. Hellman, E. H. Hartferd, P. K. Chan, *Phys. Rev. B* **46**, 1182 (1992)
- [26] G. A. Thomas, J. Orenstein, D. H. Rapkine, D. H. Capizzi, A. J. Millis, R. N. Bhatt, L. F. Schneemeyer, J. V. Waszczak *Phys. Rev. Lett.* **61**, 1313 1988
- [27] B. C. Webb, A. J. Sievers, T. Milalisin, *Phys. Rev. Lett.* **57** 1951 (1986)
- [28] I. I. Mazin, E. G. Maksimov, S. N. Rashkeev, S. Yu Savrasov, Y. A. Uspenskii, *JETP Letters* **47**, 113 (1988)
- [29] S. Uchida, K. Tamasaku, S. Tajima, *Phys. Rev. B* **53**, 14558 (1996)
- [30] F. Gao, D. B. Romero, and D. B. Tanner, *Phys. Rev. B* **47**, 1036 (1993)
- [31] J. Schützmann, B. Gorshunov, K. F. Renk, J. Münzel, A. Zibold, H. P. Geserich, A. Erb, G. Müller-Vogt, *Phys. Rev. B* **46**, 512 (1992)

- [32] Y. Yagil, F. Baudenbacher, M. Zhang, J. R. Birch, H. Kinder, E. K. H. Salje, *Phys. Rev. B* **52**, 15582 (1995)
- [33] D. B. Romero, C. D. Porter, D. B. Tanner, L. Forro, D. Mandrus, L. Mihaly, G. L. Carr, G. P. Williams, *Solid State Comm.* **82**, 183 (1992)
- [34] C. M. Varma, P. B. Littlewood, S. Schmitt–Rink, E. Abrahams, and A. E. Ruckenstein, *Phys. Rev. Lett.* **63**, 1996 (1989)

FIGURES

FIG. 1. Transport spectral function $\alpha_{\text{tr}}^2(\omega)F(\omega)$ used in the calculations.

FIG. 2. Comparison between the calculated optical conductivity (real part) $\sigma_1(\omega)$ using Eq. (67) (dashed line) and using the “extended” Drude formula, Eq. (68) (solid line).

FIG. 3. Same as Fig. 2 at low energies

FIG. 4. Transport relaxation rate $\frac{1}{\tau_{\text{tr}}^*(\omega)}$ at $T = 10$ K for different constants of coupling, $\lambda_{\text{tr}} = 0.2, 0.6, 1.0, 1.4$, and different phonon spectra with $\omega_{\text{m}} = 612 \text{ cm}^{-1}, 735 \text{ cm}^{-1}, 882 \text{ cm}^{-1}$, calculated using the “extended” Drude formula. In dimensionless units all curves fall on top of each other.

FIG. 5. Transport relaxation rate $\frac{1}{\tau_{\text{tr}}^*(\omega)}$ at $T = 10$ K and 100 K for $\lambda = 1$, $\omega_{\text{m}} = 735 \text{ cm}^{-1}$. The inset shows the one-particle relaxation rate calculated for the same parameters.

FIG. 6. Calculated reflectivity for optimally doped LSCO at $T = 300$ K, using the “extended” Drude formula with $\lambda = 2.5$, $\omega_{\text{p}} = 1.8 \text{ eV}$, $\epsilon_{\infty} = 4.6$, $1/\tau_{\text{imp}} = 100 \text{ cm}^{-1}$.

FIG. 7. FIR reflectivity for LSCO from Gao *et al* at different temperatures compared to our calculations.

FIG. 8. Same as Fig. 7 on a larger energy scale.

FIG. 9. FIR reflectivity for YBCO from Schützmann *et al* at different temperatures compared to our calculations, using $\lambda = 3$, $\omega_{\text{p}} = 3 \text{ eV}$, $\epsilon_{\infty} = 5.8$, $1/\tau_{\text{imp}} = 300 \text{ cm}^{-1}$. The inset shows the calculated curve at room temperature in a larger energy scale.

FIG. 10. Calculated transport relaxation rate $\frac{1}{\tau_{\text{tr}}^*(\omega)}$ for YBCO at different temperatures.

FIG. 11. Calculated DC resistivity for YBCO as a function of temperature.

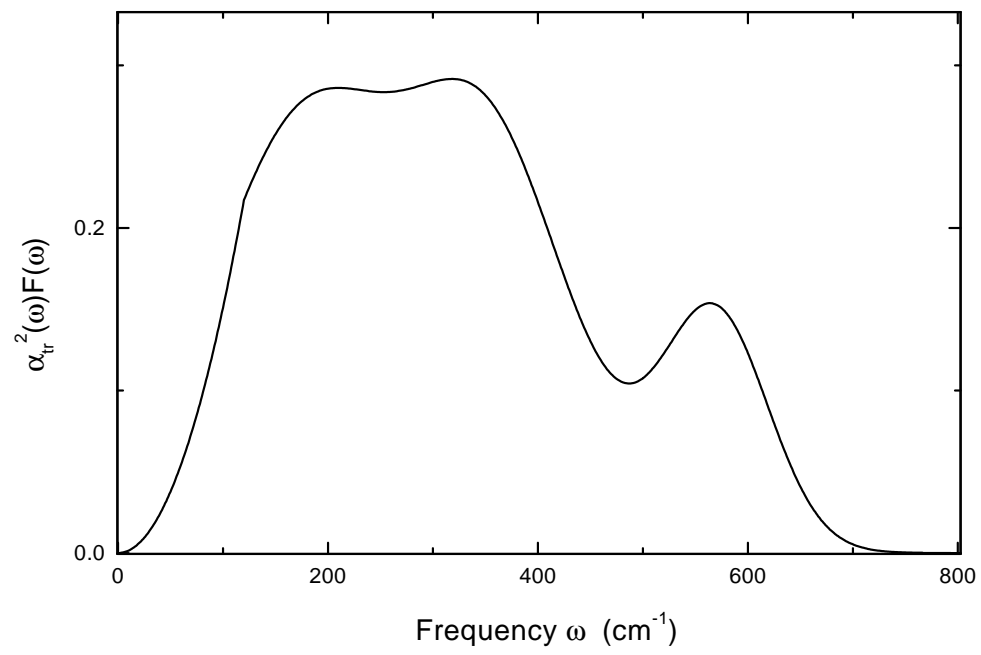


Fig. 1 Electron-phonon interaction and optical spectra of metals, Kaufmann, Maksimov, Salje

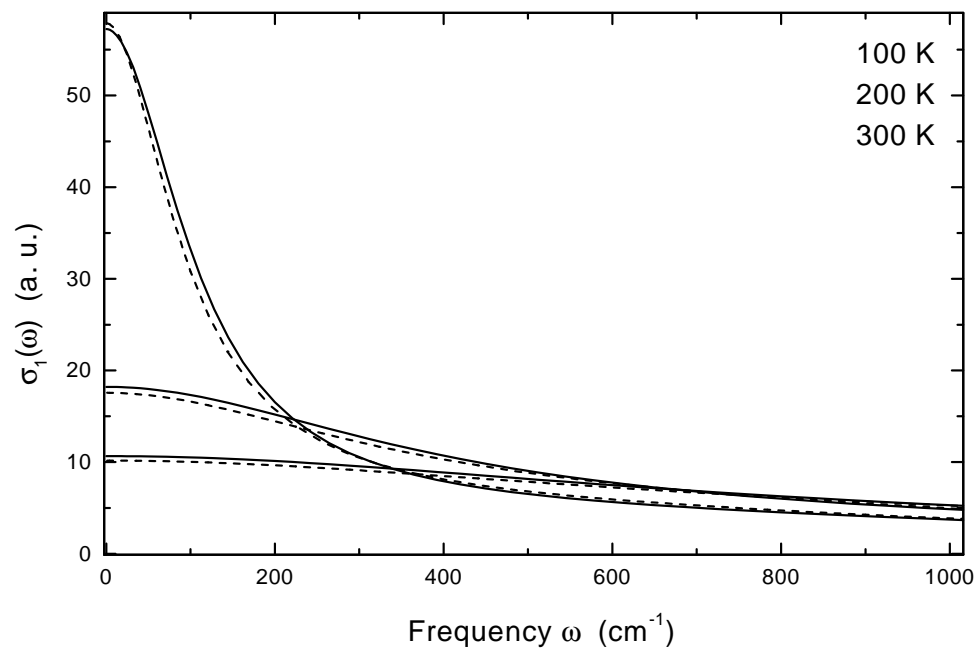


Fig. 2 Electron-phonon interaction and optical spectra of metals, Kaufmann, Maksimov, Salje

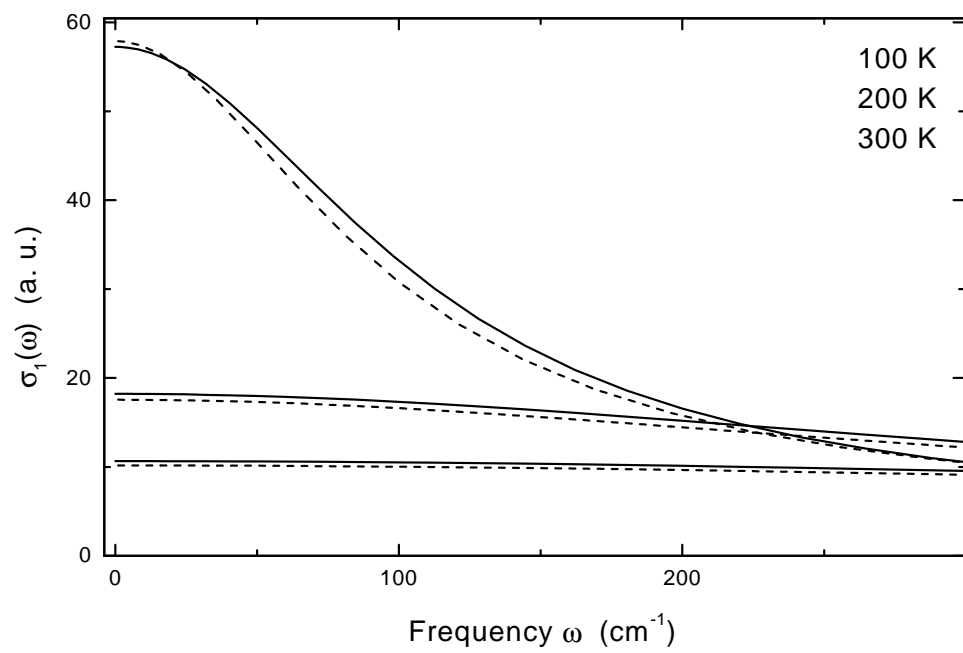


Fig. 3 Electron-phonon interaction and optical spectra of metals, Kaufmann, Maksimov, Salje

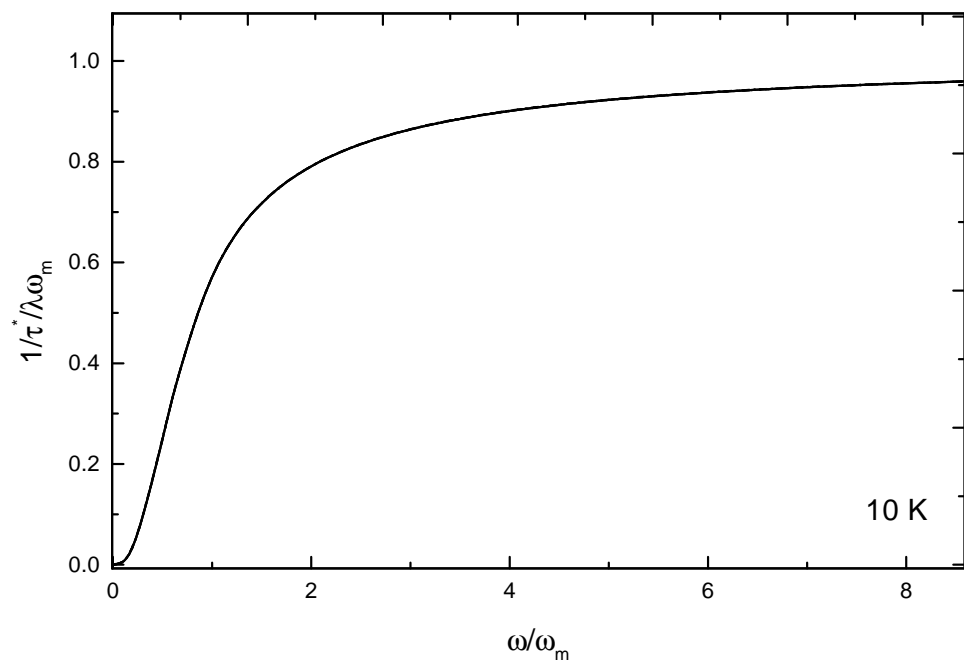


Fig. 4 Electron-phonon interaction and optical spectra of metals, Kaufmann, Maksimov, Salje

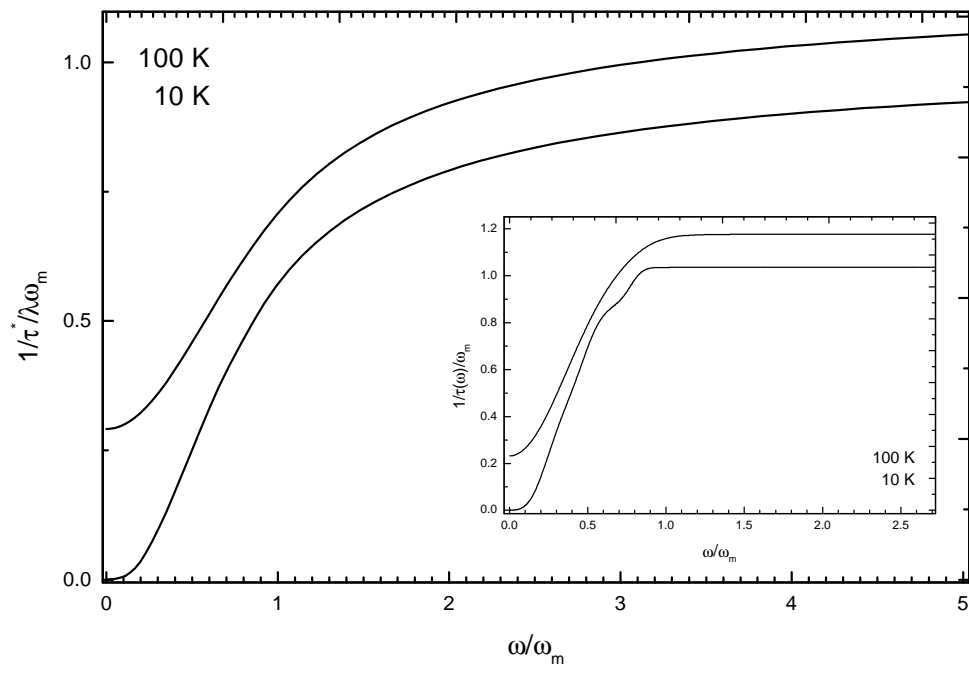


Fig. 5 Electron-phonon interaction and optical spectra of metals, Kaufmann, Maksimov, Salje

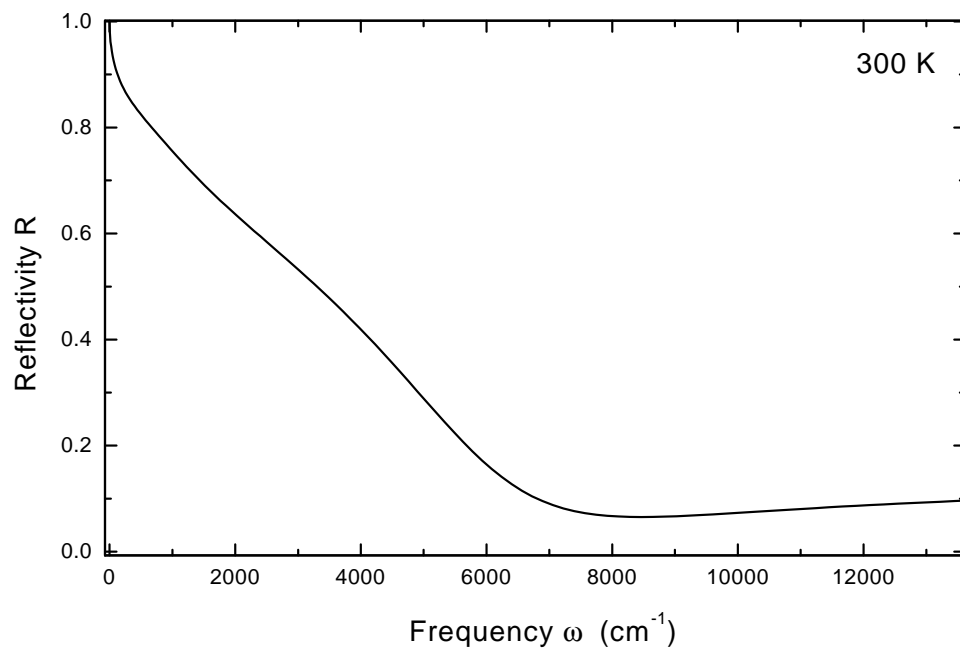


Fig. 6 Electron-phonon interaction and optical spectra of metals, Kaufmann, Maksimov, Salje

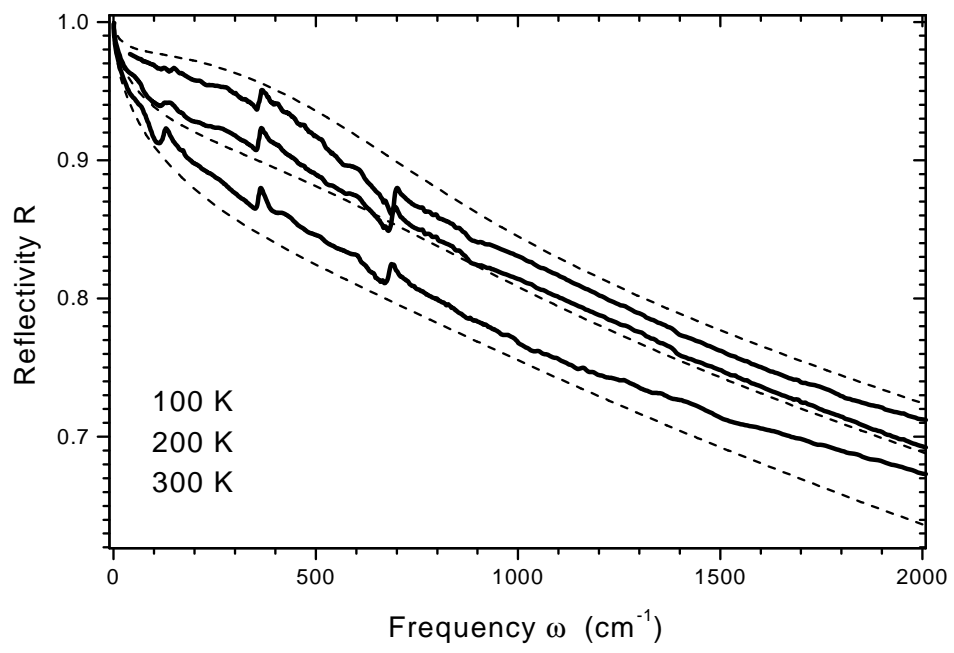


Fig. 7 Electron-phonon interaction and optical spectra of metals, Kaufmann, Maksimov, Salje

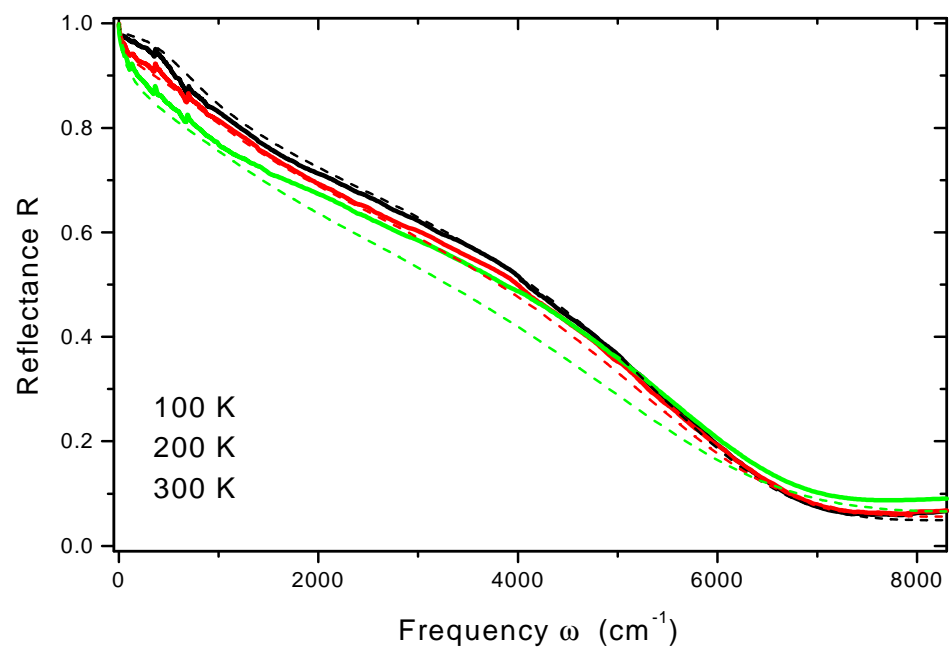


Fig. 8 Electron-phonon interaction and optical spectra of metals, Kaufmann, Maksimov, Salje

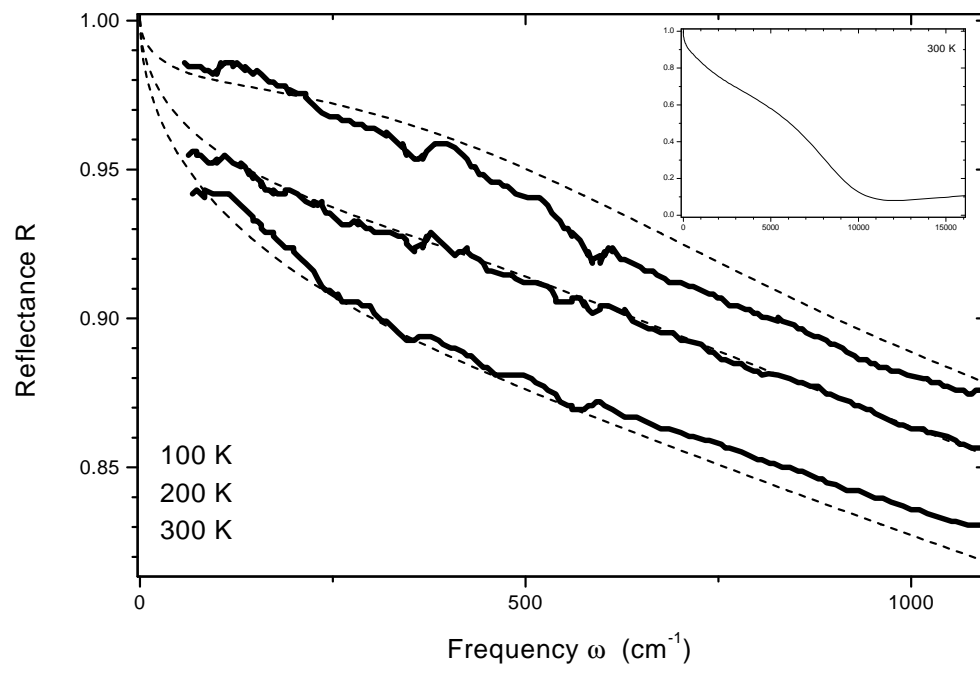


Fig. 9 Electron-phonon interaction and optical spectra of metals, Kaufmann, Maksimov, Salje

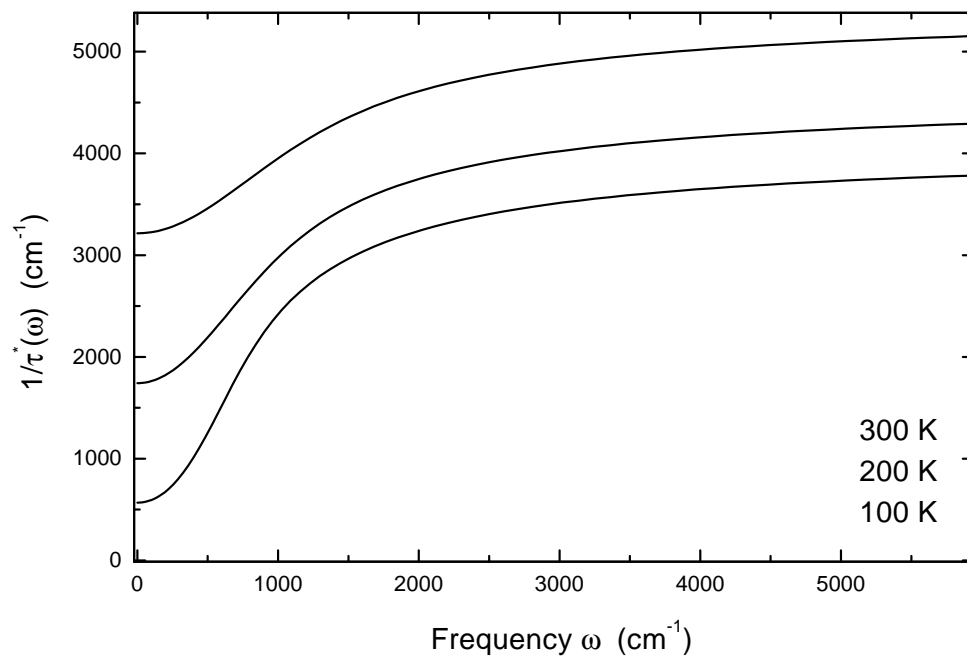


Fig. 10 Electron-phonon interaction and optical spectra of metals, Kaufmann, Maksimov, Salje

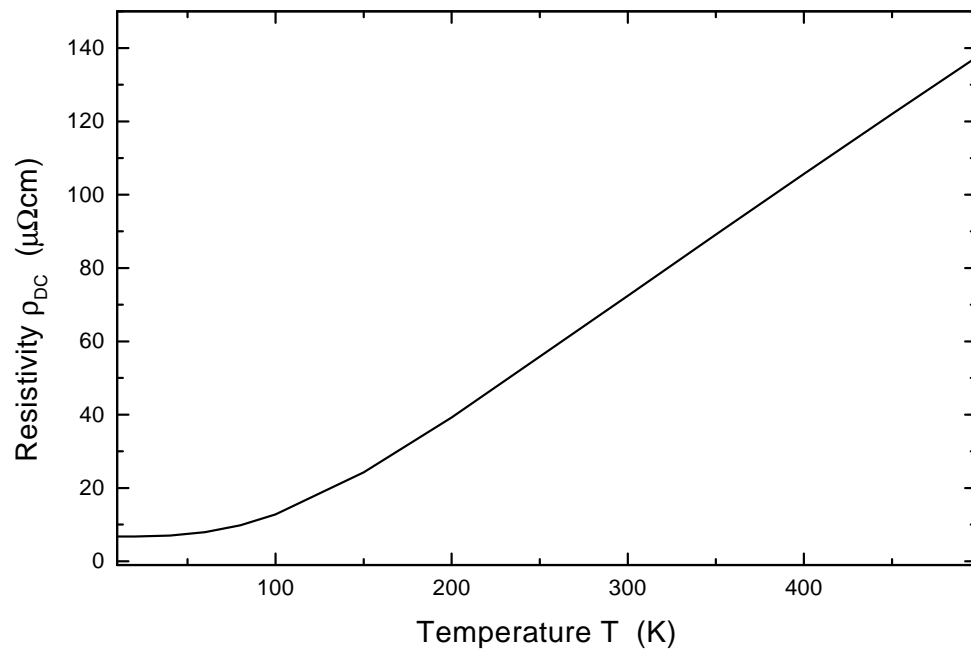


Fig. 11 Electron-phonon interaction and optical spectra of metals, Kaufmann, Maksimov, Salje